



The impact of seismic noise produced by wind turbines on seismic borehole measurements

Fabian Limberger^{1,2}, Georg Rumpker^{1,3}, Michael Lindenfeld¹, and Hagen Deckert²

¹Institute of Geosciences, Goethe University Frankfurt, 60438 Frankfurt am Main, Germany

²Institute for Geothermal Resource Management (IGEM), 55411 Bingen, Germany

³Frankfurt Institute for Advanced Studies (FIAS), 60438 Frankfurt am Main, Germany

Correspondence: Fabian Limberger (limberger@igem-energie.de)

Received: 16 January 2023 – Discussion started: 7 February 2023

Revised: 27 April 2023 – Accepted: 18 July 2023 – Published: 18 August 2023

Abstract. Seismic signals produced by wind turbines can have an adverse effect on seismological measurements up to distances of several kilometres. Based on numerical simulations of the emitted seismic wave field, we study the effectiveness of seismic borehole installations as a way to reduce the incoming noise. We analyse the signal amplitude as a function of sensor depth and investigate effects of seismic velocities, damping parameters and geological layering in the subsurface. Our numerical approach is validated by real data from borehole installations affected by wind turbines. We demonstrate that a seismic borehole installation with an adequate depth can effectively reduce the impact of seismic noise from wind turbines in comparison to surface installations. Therefore, placing the seismometer at greater depth represents a potentially effective measure to improve or retain the quality of the recordings at a seismic station. However, the advantages of the borehole decrease significantly with increasing signal wavelength.

1 Introduction

Global warming, energy crises and hence the goal to reduce the dependency on fossil energies demonstrate the relevance of exploiting renewable energies, including wind power. Thus, the increase in the number of wind turbines (WTs) plays a key role in the coming years. WTs are preferably installed in remote areas with windy conditions to increase the power production and to minimise their impacts (e.g. shadowing, acoustic noise and infrasound) on the environment. Seismic stations are often located in areas with similar con-

ditions due to the low seismic noise levels compared to urban areas with anthropogenic noise sources such as traffic, industry and railways. Nevertheless, the vibration of WTs can have a significant impact on seismic stations and networks. However, the effects strongly depend on the distance between the seismometer and the WT.

Seismic signals of WTs are characterised by frequencies between 1 and 10 Hz and have been described in detail in a number of studies (e.g. Saccorotti et al., 2011; Stammer and Ceranna, 2016; Zieger and Ritter, 2018). The systematic decays of the corresponding signal amplitudes with distance from the WT or wind farms (WFs) have been analysed at various WFs (Neuffer and Kremers, 2017; Limberger et al., 2021; Gaßner and Ritter, 2023). Analytical and numerical approaches to modelling the amplitudes have been developed in terms of considering single WTs (Gortsas et al., 2017; Lerbs et al., 2020; Abreu et al., 2022) and complete WFs (Limberger et al., 2021, 2022), including wave field interferences from multiple WTs. On this basis, methods for predicting and reducing seismic noise from WTs or other noise sources are developed taking into account, for example, meta-materials (Colombi et al., 2016; Abreu et al., 2022), interferences and topographic effects (Limberger et al., 2021, 2022), and denoising methods (e.g. Heuel and Friederich, 2022). However, effective and robust solutions to compensate the seismic noise without losing the quality of the natural seismological signals are missing. It is generally known that seismometers in boreholes have lower noise levels compared to stations at the surface (Withers et al., 1996; Boese et al., 2015), which can improve the detectability of seismic events even in urban areas (Malin et al., 2018). Boese et al. (2015) reported

a noise level reduction of up to 30 dB (average 10 dB) on a 383 m deep borehole sensor compared to a surface sensor for frequencies ≥ 1 Hz. Similar effects of borehole installations on signals from WTs are shown by Zieger and Ritter (2018). They compared signals measured in boreholes with surface data and showed a significant reduction in the surface wave amplitude induced by a nearby WF. Neuffer and Kremers (2017) analysed data from borehole stations as well but did not systematically study the relationship to surface data. Nevertheless, they estimated a noise reduction by an order of magnitude due to the borehole installation. Obviously, borehole installations can play a relevant role in reducing the noise of WTs at seismometers. However, their capabilities and limitations and the predictability of their effectivity have not been studied in detail.

Here, we investigate the effectivity of borehole installations using numerical simulations. We perform sensitivity studies on depth-dependent signal amplitudes in view of signal frequencies, seismic velocities, homogeneous and layered subsurface structures, attenuation, and the distance between sources and receivers. We compare our numerical results with data from borehole measurements reported by Zieger and Ritter (2018). Our results provide constraints on the distances between WTs and seismic stations necessary to reduce the noise levels to a desired level.

2 Model set-up and data processing

2.1 Description of the numerical model

The forward modelling of the wave propagation is performed in two dimensions (x - z plane) using the software package Salvus (Afanasiev et al., 2019), which enables the simulation of the complete wave field (P wave, S wave and surface waves, including conversion and scattering effects). A comparison of the results with a simulation in three dimensions shows that a two-dimensional approach seems sufficient for addressing the problem described (the corresponding data are in Fig. S1 in the Supplement). The seismic source is located at the surface of the model domain (Fig. 1). The source wavelet is a tapered sinusoidal function with a length of five signal periods, which implies that the source duration increases for simulations with lower frequencies. The exciting force is assumed to be vertically oriented. The modelling domain has a length of 8 km (x direction) and a depth of 2 km. Absorbing boundaries are added to all sides, except for the free surface on top of the model. The absorbing boundary has a minimum thickness of 2 times the maximum wavelength used during the simulation to sufficiently suppress reflections at the sides. A synthetic 1 km deep borehole is located at a distance of 4 km from the source. Receivers are located at intervals of 10 m along the borehole to extract the synthetic seismograms at 101 positions. In this work, we study the effects of both homogeneous and layered models,

including effects of varying seismic velocities. The velocity of the P wave is calculated from $V_P = 1.7 \times V_S$, and the density is 2600 kg m^{-3} in every simulation. The source frequency is systematically increased from 0.2 to 6 Hz (step size of 0.2 Hz) to cover a wide range of typical signal frequencies observed for WTs (see references). Signals at about 1 Hz and between 3 and 4 Hz are widely observed by seismometers close to WTs. These frequencies are related to the tower eigenmodes of a WT (Zieger and Ritter, 2018; Zieger et al., 2020) and depend on the type and specifications of the WT. Hence, instead of choosing just a few specific frequencies corresponding to one specific wind turbine type, we keep the approach universal and study various frequencies between 0.2 and 6 Hz. A separate simulation is performed for each frequency and model. The grid spacing is generated using three elements per minimum wavelength to avoid numerical artefacts. All studied models are listed in Table 1. Models 1–9 are used to study general effects of seismic velocities, geological layering and attenuation. Model 10 is generated based on results from the MAGS2 project (Spies et al., 2017), which provided detailed information on the seismic velocities in the region of Landau in Rhineland-Palatinate, Germany. We use this information about the local subsurface to establish a corresponding average-velocity model (Fig. S2) and to perform the real-data validation of our proposed solutions.

2.2 Post-processing of the synthetic seismograms and comparison to analytical solutions

For each single simulation, synthetic seismograms (or traces) are extracted at every receiver location in the synthetic borehole (grey lines in Fig. 2). The maximum amplitude for each trace (vertical component) is obtained to derive a frequency-dependent relationship between signal amplitude and depth (red line in Fig. 2). The frequency-dependent amplitudes with depth are normalised to the amplitude at the surface. Finally, the interpolation of the resulting data shows the spectral amplitudes depending on the borehole depth (Fig. 3a).

As a benchmark, we compare the numerical results with two analytical solutions (Fig. 3b). The first solution (coloured interpolation in Fig. 3b) is based on a formulation of Barkan (1962)

$$A_z = \left(-0.2958e^{-\frac{(0.8474)2\pi z}{\lambda}} + 0.1707e^{-\frac{(0.3933)2\pi z}{\lambda}} \right), \quad (1)$$

where the amplitude of the vertical ground motion A_z at depth z is a function of wavelength λ and z . The second analytical solution (dashed black lines in Fig. 3b) is the estimation of the Rayleigh wave penetration depth using various wavelength approximations (λ , $\lambda/2$, $\lambda/3$). Usually, a fraction of λ ($\lambda/2$ or $\lambda/3$) is used to estimate the penetration depth of surface waves. However, this likely underestimates and neglects the amplitudes at depth. For example, $\lambda/3$ exhibits a reduction of about 10% and $\lambda/2$ a reduction of 30%, which implies that this simple approximation is inadequate to derive the frequency-dependent amplitudes as a

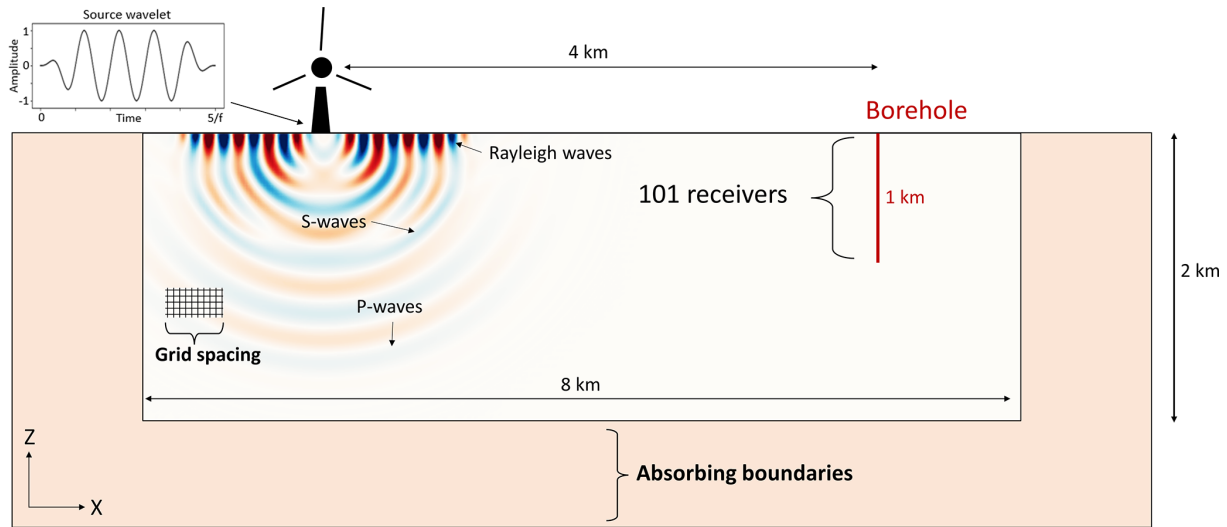


Figure 1. The numerical model includes a sinusoidal source wavelet, receivers located along a line from the surface to a depth of 1 km and a sufficient grid spacing (three elements per minimum wavelength of the simulation) as well as absorbing boundaries (2 times the maximum wavelength of the simulation). P waves, S waves and surface waves are simulated during the forward modelling. Synthetic seismograms are extracted at positions indicated by the red line (borehole).

Table 1. List of models used in this study. Models 1–9 are generic to study the effects of geophysical parameters and layers in the subsurface. Model 10 is used for the validation with real data. The quality factor Q describes the loss of energy per seismic wave cycle due to anelastic processes or friction inside the rock during the wave propagation. The damping of the P wave and S wave decreases with increasing Q_P and Q_S .

ID	Description	V_{S1}	V_{S2}	V_{S3}	V_{S3}	V_P
Model 1	Homogeneous half-space	500	–	–	–	$1.7 V_S$
Model 2	Homogeneous half-space	1000	–	–	–	
Model 3	Homogeneous half-space	1500	–	–	–	
Model 4	Two layers ($z = -200$ m), low velocity	500	1000	–	–	
Model 5	Two layers ($z = -200$ m), mid-velocity	1000	1500	–	–	
Model 6	Two layers ($z = -200$ m), high velocity	2000	3000	–	–	
Model 7	Three layers ($z_1 = -200$ m, $z_2 = -400$ m)	500	1000	1500	–	
Model 8	Two layers ($z = -200$ m), weak attenuation	Model 4 including $Q_S = 100$, $Q_P = 200$				
Model 9	Two layers ($z = -200$ m), strong attenuation	Model 4 including $Q_S = 30$, $Q_P = 60$				
Model 10 (Fig. S2)	Landau model (real-data validation), four layers, no attenuation ($z_1 = -200$ m, $z_2 = -400$ m, $z_3 = -600$ m)	450	750	900	1150	

function of depth. For example, Hayashi (2008) and Kumagai et al. (2020) claim that surface wave penetration depth is down to a depth between $\lambda/4$ and $\lambda/2$, whereas $\lambda/3$ is often chosen to be the most suitable assumption (e.g. Larose, 2005). The analytical solutions are generally based on the interplay of seismic velocity v , frequency f and wavelength λ :

$$\lambda = v/f. \tag{2}$$

3 Results

3.1 Homogeneous models

The comparison between analytical and numerical solutions (Fig. 3) applied to a homogeneous half-space model shows very similar results for the amplitude–depth relationships per frequency. This implies that on the one hand the numerical simulation reliably reproduced the analytical calculations.

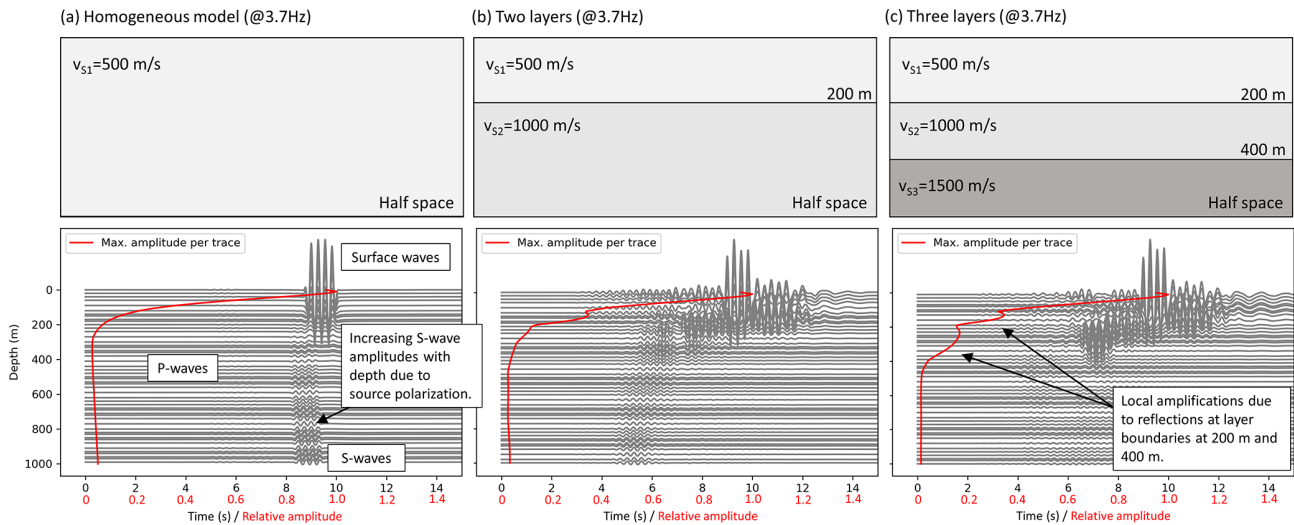


Figure 2. Example of the synthetic seismograms (grey lines) depending on the depth for signals at 3.7 Hz. The values of the red line are calculated from the maximum amplitude per trace, which is affected by layers in the subsurface. The values of the red lines are then normalised to the amplitude at the surface. Hence, the red values of the x axis (from 0 to 1.4) are amplitudes and can be assigned to the red line, and the black values (from 0 to 14) are the time and can be assigned to the waveforms. P-, S-, and Rayleigh waves are simulated. The surface wave dominates the wave field near the surface.

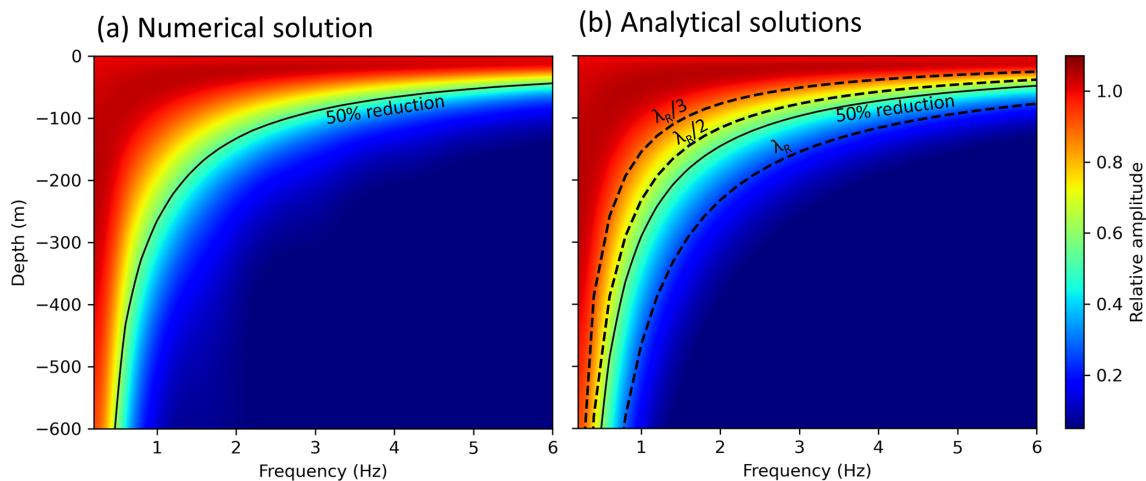


Figure 3. Benchmark comparison between numerical solutions and analytical solutions (λ estimations, dashed lines) for homogeneous models, based on the formulation in Barkan (1962). The results are very similar, which proves the reliability of the numerical solution for this simple benchmark. The difference between (a) and (b) is shown in detail in the Supplement (Fig. S4).

On the other hand, an analytical solution might be sufficient if the subsurface is approximately homogeneous. The estimation of the Rayleigh wave penetration depth fits very well to the more complex analytical solution (Fig. 3b); however, the fraction of λ should be chosen, carefully considering the preferred reduction in noise with depth. These analytical solutions are limited regarding complex models of the subsurface.

Generally, a borehole should be deeper to yield a reduction in low-frequency seismic noise (e.g. 1 Hz) compared to high frequencies (> 4 Hz). This is expectable since the wave-

length of a wave with a low frequency is larger compared to high frequencies. Consequently, the penetration depth of the surface wave is deeper. In view of Eq. (2) the seismic velocity impacts this relationship. The effects of the seismic velocity, signal frequency, layers in the subsurface and attenuation on the depth-dependent amplitudes are simulated using homogeneous and layered models (Fig. 4). In the case of high seismic velocities in the subsurface, deeper boreholes are required to yield a sufficient noise reduction. Furthermore, from the simulation results we obtain the effect of the signal frequency on the amplitudes. We find, for example,

that a borehole should be 100 m deep to reduce the noise of 3 Hz signals at 4 km distance to the WT by 50 % if the velocity of the S wave is 500 m s^{-1} (Fig. 4a), but the same borehole should be about 280 m deep for a velocity of 1500 m s^{-1} (Fig. 4c).

3.2 Layered models

In the case of a layered subsurface, we find that the amplitude decay with depth is dominated by the top layer, which (here) has a thickness of 200 m. The comparison between Fig. 4d and g shows that a third deep layer with a high velocity has no significant impact on the results. However, again, the estimation of sufficient borehole depths depends strongly on the seismic velocity of the layers (especially the top layer). A borehole with a depth of 200 m seems to be sufficient if the S-wave velocity of the top layer is approximately 500 m s^{-1} (Fig. 4d), but this is not true if the velocity is increased (Fig. 4e, f). Signals $> 4 \text{ Hz}$ can be suppressed significantly in any case, but signals below this frequency (e.g. at 1 Hz) are not sufficiently affected by boreholes surrounded by rock with high seismic velocities. Hence, the geological setting and the seismic velocities play a key role concerning the evaluation of the effectivity of a borehole installation that aims to reduce the seismic noise produced by WTs.

We further study the effect of attenuation (absorption) by specifying Q_S and Q_P . In model 8 (Fig. 4h), we used relatively high Q values ($Q_S = 100$ and $Q_P = 200$) (Eulendorf and Wegler, 2016) for a weak attenuation (e.g. compact rock), and in model 9 (Fig. 4i) we used relatively low Q values ($Q_S = 30$ and $Q_P = 60$) to simulate a strong attenuation (e.g. near-surface sedimentary rocks). We find that the general amplitude–depth relationship is not significantly affected by attenuation compared with the same model without attenuation (model 4). There are some frequency-dependent effects (e.g. at 4 Hz) showing slightly increased amplitudes below a depth of 200 m in the case of strong attenuation (A in Fig. 4i). This can be explained by a reduced contrast between the amplitude at the surface and the amplitude at depth. A strong attenuation causes generally lower amplitudes compared to a scenario without attenuation; however, the contrast between the amplitude in the borehole relative to the surface seems to be weakened.

3.3 Effect of distance between WT and seismic station

The frequency-dependent amplitude decay with depth is generally affected by the distance between the WT and the borehole. To simulate these effects regarding the vertical and horizontal ground motion, we use model 4 (two layers with low velocities; see Table 1) and decrease the distance between the source and the receivers systematically from 4 to 1 km. The results are presented in Fig. 5. With decreasing distance between the source and the borehole, amplitudes increase at frequencies between 2 and 4 Hz up to a depth of 200 m, es-

pecially regarding the horizontal component in the x direction of the model. This indicates relatively strong effects at the base of the topmost layer at 200 m depth, likely due to strong reflection concerning the specific frequencies. These effects might change in the case of higher velocities or a change in frequency or thickness of the top layer. Furthermore, we observe that the amplitude of the horizontal component is decreasing much faster with depth compared to the vertical component. This behaviour can be described analytically (Barkan, 1962). However, layers in the subsurface can have an adverse effect for specific frequencies, as described. The layer boundary at 200 m depth seems to isolate the amplitudes above and below. This means that a borehole could be very effective at depths $> 200 \text{ m}$, at least for this specific case.

3.4 Effects of attenuation

To investigate the effect of attenuation on the effectivity of a borehole for a specific frequency, we use model 4 including weak and strong attenuation. In this case, we study signals of 3.7 Hz (which is a typical frequency emitted by WTs), calculate the seismic radiation in the x – z plane and compare the results to those for the model without attenuation. As expected, we find that a strong attenuation affects the general amplitude decay with distance to the source and with depth (Fig. 6a, c, e). However, the relative amplitudes between depth and the surface are only slightly affected by attenuation. This becomes obvious by looking at the almost identical results when the amplitudes at depth are normalised to the corresponding amplitude at the surface (Fig. 6b, d, f). The tendency is that the contrast of amplitudes at the surface compared to amplitudes at depth is lower when strong attenuation exists (Fig. 6f). This implies that a borehole in a strongly attenuating environment might not be as effective as in less attenuating rock. However, the attenuation is not the dominating parameter to evaluate the effectivity of the borehole installation, as shown before. It should be noted that the undulation in the x direction is due to the layering (reflection effects).

With this analysis we can evaluate the distance of a seismometer to the WT. In view of Fig. 6c, we show that the distance between the seismometer and the WT could be reduced from 4 to 2 km if the seismometer is placed in a 100 m deep borehole, thus avoiding a significant increase in the noise level. But it should be clear that this is only an estimation for the specific case in this study and is very likely affected by changes in seismic velocity and the structure of the subsurface.

3.5 Real-data validation

In this section, we validate the presented approach with data from seismic borehole installations. Close to the city of Landau in the upper Rhine Valley, two seismic borehole stations

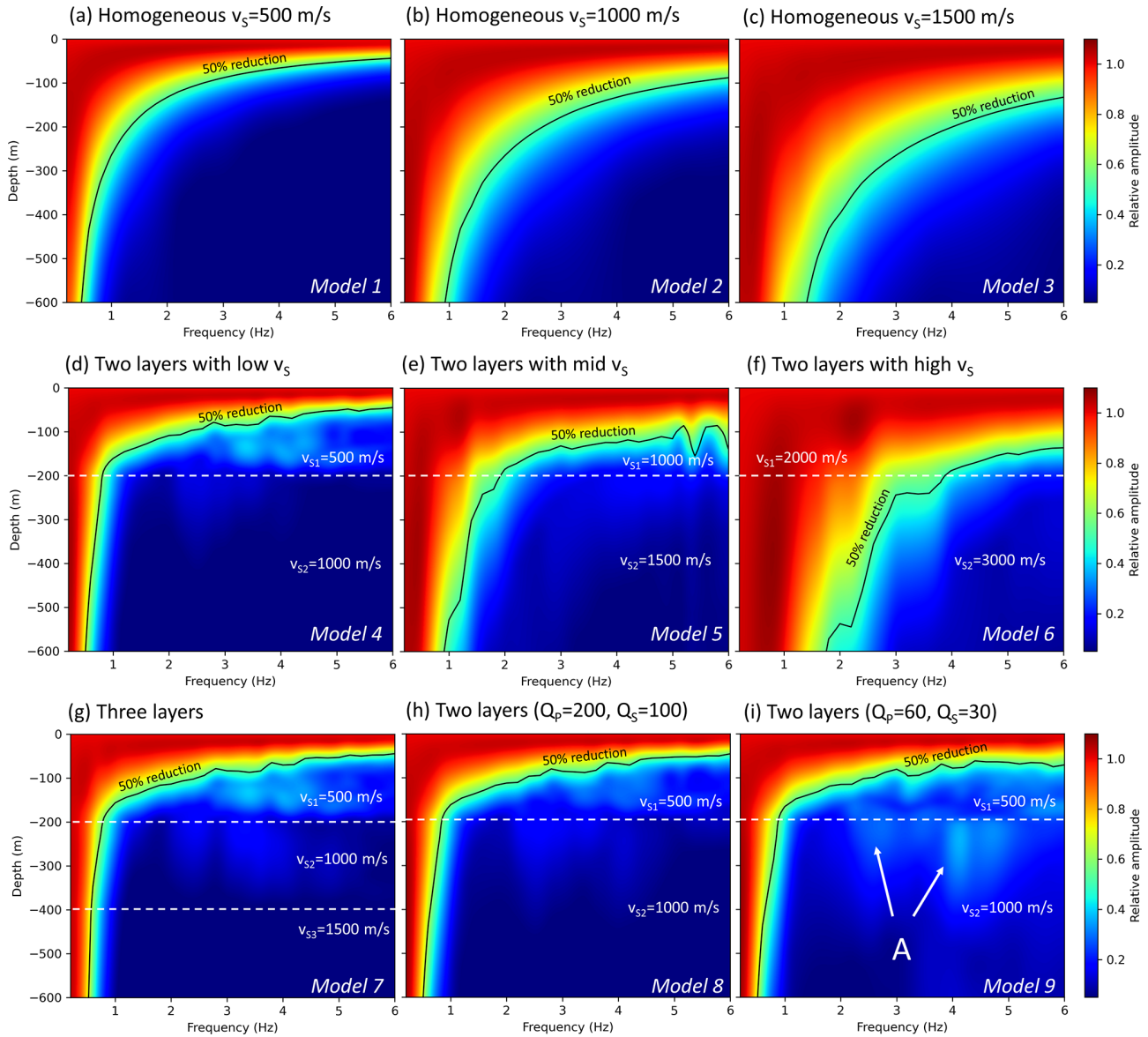


Figure 4. Effect of various models (a–c: homogeneous; d–g: layered; h, i: with attenuation) on the frequency-dependent amplitude decrease with depth. The dashed white lines denote the layer boundaries. The solid black line indicates the amplitudes of 50 % reduction compared to the corresponding amplitude at the surface. The results are extracted from synthetic seismograms at 4 km distance from the source. Amplitudes as a function of frequency are normalised to the corresponding amplitude at the surface.

at depths of 305 m (ROTT station) and 150 m (LDE station) are located at distances of approximately 5.5 km (ROTT) and 3.8 km (LDE), respectively, to the next WTs (Fig. 7). These permanent stations are part of the earthquake monitoring system of the geological survey in Rhineland-Palatinate, Germany. Zieger and Ritter (2018) temporarily measured the frequency-dependent noise of the nearby WTs at the surface of the corresponding borehole locations and calculated power spectral densities (PSDs) (Fig. S3). They showed a clear reduction in measured noise due to the boreholes. We took the PSD values of Zieger and Ritter (2018) and trans-

formed the data into relative ground motions. At frequencies of 1 Hz, we find an amplitude reduction of 73 % at the ROTT borehole station. At LDE we observe a reduction of 34 % for 1 Hz signals and 71 % for 3.7 Hz signals by comparing the amplitudes of the borehole seismometer with the surface amplitudes (Fig. S3). The signals with 3.7 Hz are not reliably observable at ROTT and are therefore not included in further analysis. These factors of amplitude reduction are used as a reference for numerical results in our study. A numerical model (Fig. 8a) is built using subsurface information derived from the MAGS2 project (Fig. S2) (Spies et al., 2017), which

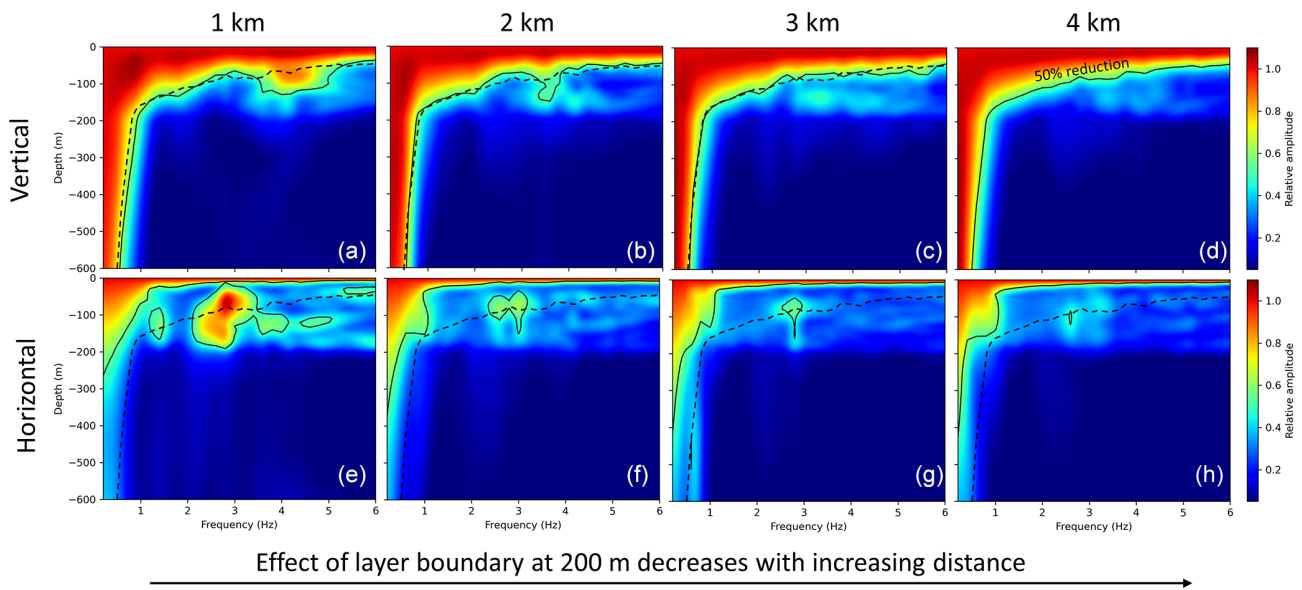


Figure 5. Effect of distance between source and borehole on vertical (z axis) and horizontal (x axis) seismogram components. Model 4 is used for these simulations, which means that the results in (d) are identical to Fig. 4d. The 50 % reduction in (d) is indicated by the dashed black line in all other figures for reference. The distance has an effect on the amplitudes with depth, especially regarding the horizontal components. The layer boundary at 200 m depth isolates the amplitudes above and below this layer. Amplitudes as functions of frequency are normalised to the corresponding amplitude at the surface.

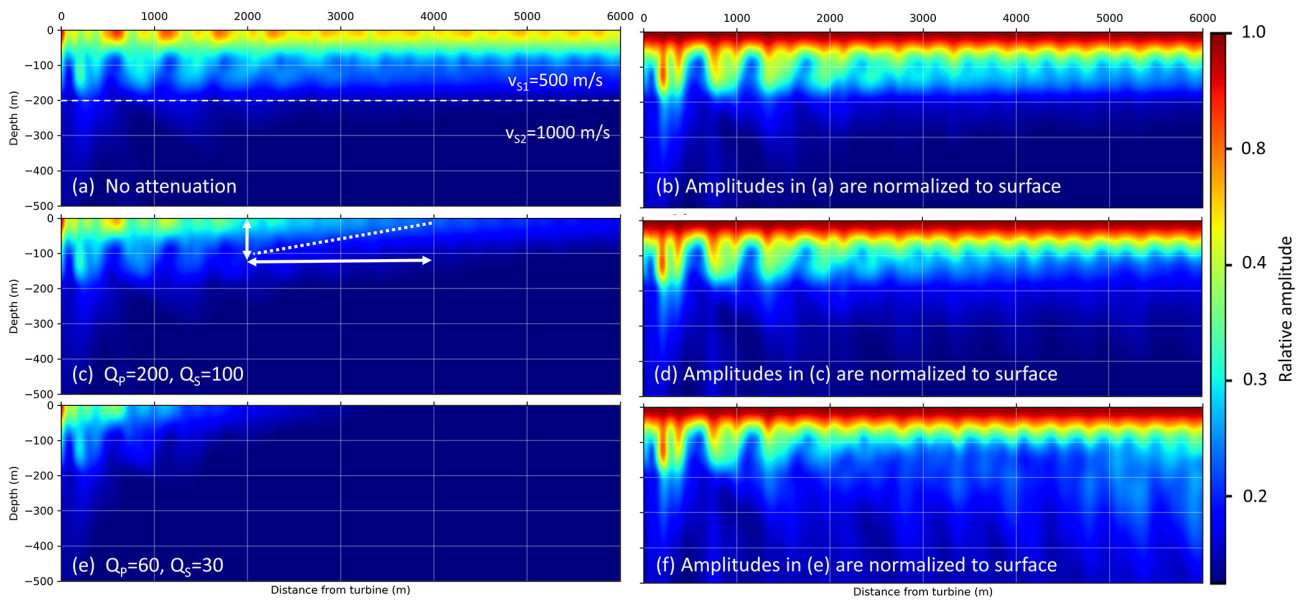


Figure 6. (a, c, e) Effect of attenuation on amplitude decays, normalised to source amplitude. (b, d, f) Amplitudes are normalised column-wise, which means that at each distance in the x direction, the amplitude with depth is normalised to the corresponding amplitude at the surface. The dominant signal frequency in these simulations is 3.7 Hz.

provides detailed seismic velocities and is hence one of the most accurate velocity models of the Landau region. The model of the local subsurface contains relatively low seismic velocities due to the younger sediments in the upper Rhine Valley. The model we extracted has four layers with increasing S-wave velocities of 450 m s^{-1} (top layer), 750 m s^{-1}

(second layer), 900 m s^{-1} (third layer) and 1150 m s^{-1} (half-space). Again, the density is fixed at 2600 kg m^{-3} , and the P-wave velocity is 1.7 times V_S . The synthetic boreholes in the numerical models are correspondingly located at distances of 3.8 km (LDE) and 5.5 km (ROTT), respectively, to the source point. From the simulations (Fig. 8b and c), we

can calculate the spectral isoline of an amplitude reduction of 73 % (ROTT) and the isoline of 71 % and 34 % (LDE) for all frequencies between 0.2 and 6 Hz. Based on the model of the subsurface, a comparison of the numerical results with the observed data from Zieger and Ritter (2018) shows good agreement and thus validates our amplitude estimations. The model is characterised by a first significant layer boundary at 200 m depth, where the S-wave velocity increases from 450 to 750 m s⁻¹. Interestingly, this layer boundary significantly affects the amplitude decrease with depth, especially regarding signals with a frequency between 2 and 4 Hz. This effect is likely due to reflections of the waves that are mainly travelling along the top layer. Considering these effects, the observed amplitude reduction of 71 % in the 3.7 Hz signals can only be reproduced numerically by the layered model and would fail for a homogenous model. The observed reduction of 34 % in the 1 Hz signals at the LDE borehole station is also accurately described by our modelling. The reduction of 73 % in the 1 Hz signals at ROTT is simulated appropriately. However, there is a discrepancy between observed and simulated amplitude reductions at a depth of 305 m (ROTT). In this frequency range (around 1 Hz), the amplitude decay with depth is very sensitive and thus challenging to perfectly fit.

4 Discussion and conclusions

In this work, we study the effectivity of borehole installations to reduce the impact of seismic noise produced by WTs on seismological recordings. Based on numerical models, the effects of geophysical parameters, such as seismic velocities and attenuation, and layering of the subsurface are simulated to constrain the depth of seismic borehole stations and significantly reduce the noise produced by WTs.

We validate our approach by comparisons with existing real data published by Zieger and Ritter (2018). We can reproduce the observed reduction factors by Zieger and Ritter (2018) of signal amplitudes at specific frequencies measured at the surface and at depth at two boreholes close to Landau in Rhineland-Palatinate, Germany (Fig. 8). We point out that this validation is based on simulations using a realistic model of the subsurface which consists of three layers above a half-space (based on results given in Spies et al., 2017). Interestingly, we would not be able to explain some of the observations if the layer boundary at 200 m were not included in the model. This indicates that simplified analytical solutions (homogeneous half-space model) fail to simulate the wave field sufficiently. To increase the reliability and to enable a wider application of the method, further borehole data, covering a broad range of frequencies, are necessary and should be studied in the future. Our real-data validation is performed for the upper Rhine Valley, which is characterised by thick, relatively young sediments with low seismic velocities (Fig. 8a). Similar simulations could be performed for other geological settings characterised by more compact rock types.

The numerical modelling shows that the effectivity of such boreholes in reducing surface-generated seismic noise strongly depends on the interplay of signal frequency, seismic velocity and wavelength (Fig. 4). Low-frequency signals and high seismic velocities yield a large wavelength, which results in a penetration depth of > 600 m for the most prominent surface waves. In regions with soft sediments, boreholes of a few hundred metres depth are likely effective in reducing the noise from WTs, especially in view of the high-frequency signals. A borehole of only 200 to 300 m depth can reduce the noise of signals between 2 and 6 Hz by more than 50 %. However, boreholes might not be effective in other regions where more compact rock types and relatively high seismic velocities dominate. The typical frequency range of signals produced by WTs is between 1 and 10 Hz. The reduction in signals with frequencies around 1 Hz seems challenging due to the relatively large wavelength. These waves travel generally very far in distance and depth. Nevertheless, Zieger and Ritter (2018) demonstrated the reduction in such signals of 73 % in a borehole of 305 m depth (5 km to the next WF) and 34 % in the case of 150 m depth (3.8 km to the next WF). We confirmed these observations with our modelling (Fig. 8).

The comparison of results for homogeneous models and layered models shows that the amplitude–depth relationship is dominated by the top layer, but this depends again on the general wavelength of the surface waves and the thickness of the top layer (Fig. 4). We studied these effects for a top layer of 200 m thickness, which is characteristic of the upper Rhine Valley. The effects of various thicknesses and lateral heterogeneities (such as fault structures or site effects) could be part of future modelling studies. Moreover, additional structural measures (e.g. filled trenches) as studied by Abreu et al. (2022) could be included in the simulation to incorporate the noise-reducing effects due to boreholes as well as structural measures.

We further show that borehole installations in geological environments with strong attenuation might not be as effective as in environments with weak attenuation. Attenuation reduces the amplitude with distance in general, but it does not affect the relative amplitudes at the surface and at depth significantly (Fig. 6).

We show that the effects of the layer boundary at 200 m depth on the wave field increase with decreasing distance to the source, especially regarding the horizontal components of the signal (Fig. 5). In our simulations we apply vertically polarised source mechanisms to model the signals from the WTs. This is an approximation of the up-and-down movement of the foundation of the WT. However, other source mechanisms and polarisations might have additional effects on the wave propagation and should be part of future research. A time-limited wave package is a sufficient approximation of the source signal and a practical solution to numerically simulate effects of the subsurface on the wave propagation. However, WTs usually emit continuous signals, which might lead to additional complex wave reflections and in-

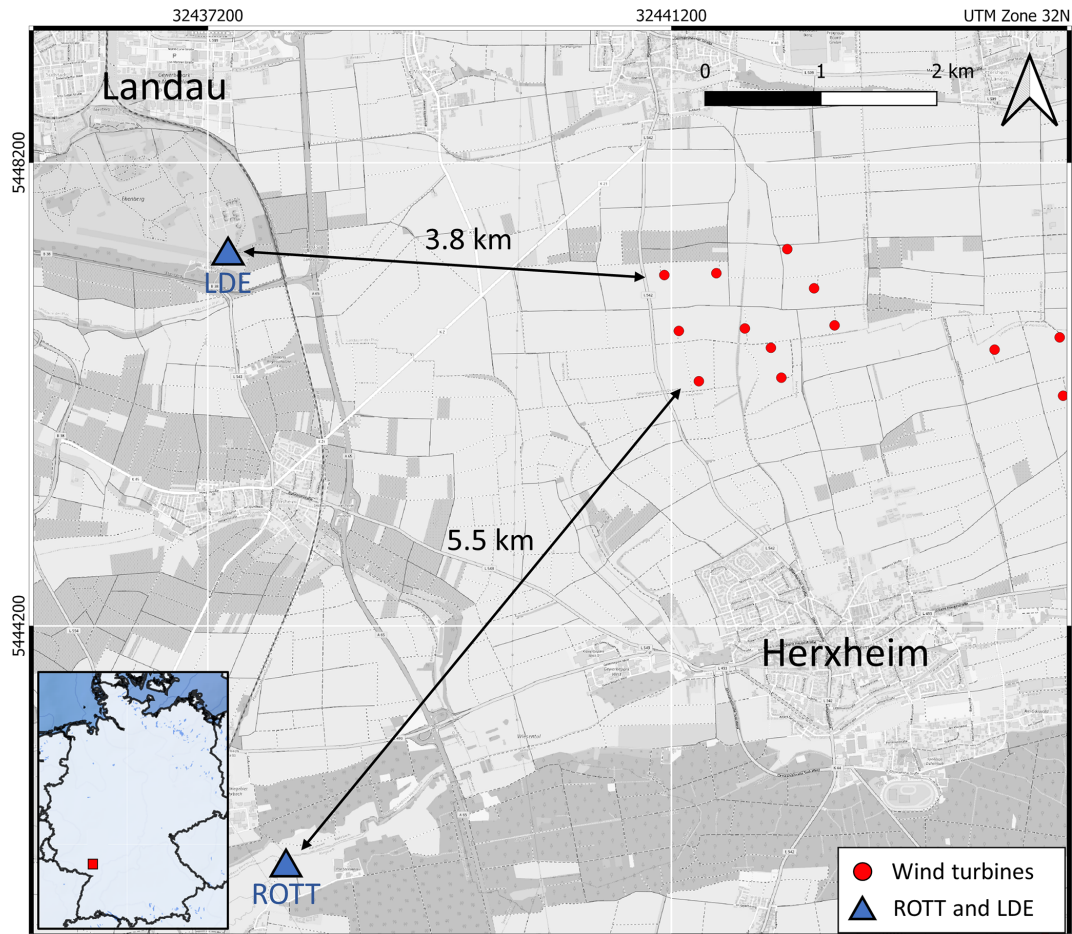


Figure 7. Map of the Landau region with borehole stations ROTT and LDE and the nearest wind farm north of Herxheim. Zieger and Ritter (2018) set up two seismic stations at the top of the boreholes to compare signal amplitudes measured at the surface with amplitudes measured at the borehole stations. (Maps: © OpenStreetMap contributors 2023. Distributed under the Open Data Commons Open Database License (ODbL) v1.0).

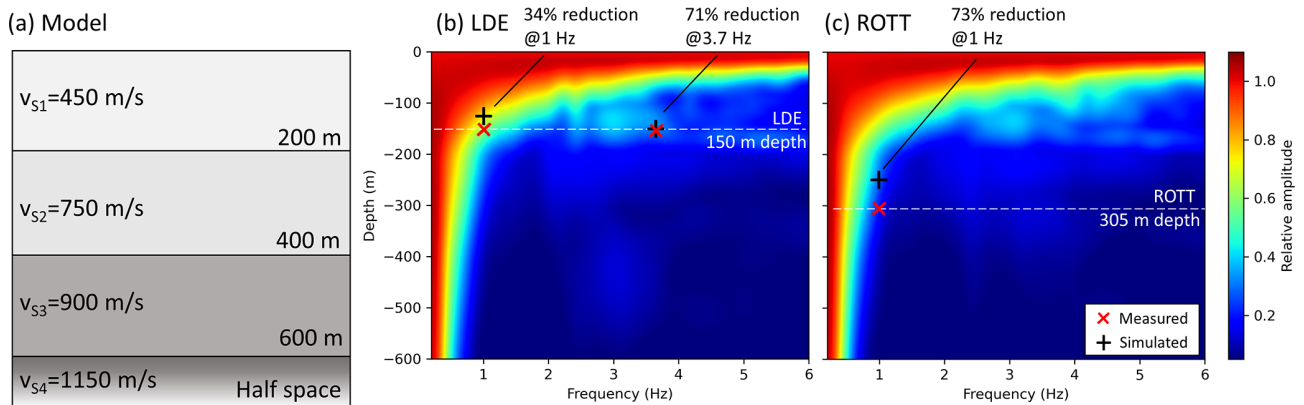


Figure 8. (a) A model with three layers above a half-space is used for the real-data validation. The model is based on information provided by the MAGS2 project (Spies et al., 2017). The results of the simulations (black crosses) are compared to observations (red plus signs) made by Zieger and Ritter (2018) and show good agreement. This means that the reduction in noise amplitudes can be reliably estimated using 2D numerical simulations.

terferences in the subsurface. Further signal modulation can also occur by wave field interferences from multiple WTs, as shown by Limberger et al. (2022).

A key aspect in evaluating the effectivity of a borehole is the general purpose of a specific seismic station. If a station is used for the detection and localisation of local earthquakes with a relatively high frequency (e.g. higher than 5 Hz), a borehole can be very effective in reducing the noise from WTs nearby. However, if the seismometer is used to measure signals with lower frequencies (e.g. 1 Hz in the case of teleseismic signals), then borehole installations might fail in reducing the noise, or the necessary borehole would require a depth that is too large to be feasible. Obviously, if signals from surface waves are to be measured, a borehole would not be the appropriate choice to reduce the impact of wind turbines; however, in this case alternative techniques such as noise filters based on machine learning (e.g. Heuel and Friederich, 2022) could help to increase the signal quality. Generally, filter techniques could affect the waveform and signal amplitude of the desired signal and should be considered carefully concerning their application. Combinations of both sensors in boreholes and advanced filter techniques could also be considered. In view of our results, we strongly recommend performing estimations based on the specific characteristics of the location of interest and not generalising and applying one estimation for all locations and seismic stations. However, besides WTs, our approach can also be applied to other anthropogenic noise sources (e.g. in urban areas) and enables a universal assessment of seismic noise and its effect on borehole installations.

To conclude, the impact of seismic noise produced by WTs on seismometers can be decreased if the seismic sensor is installed within a borehole at an adequate depth. But this strongly depends on various geophysical and geological parameters, such as seismic velocities or layering in the subsurface, and should be carefully evaluated for every geological environment separately. With this study, we provide a robust approach to perform reliable estimations of the effectivity of borehole installations.

Code and data availability. The numerical simulations were performed using the commercial software package Salvus (<https://mondaic.com/docs/0.12.13/installation>, Afanasiev et al., 2019). The simulation scripts are available from the corresponding author (limberger@igem-energie.de) on request. The data processing was performed using the Python packages NumPy (<https://numpy.org/install/>, Harris et al., 2020) and SciPy (<https://scipy.org/install/>, Virtanen et al., 2020).

Supplement. The supplement related to this article is available online at: <https://doi.org/10.5194/se-14-859-2023-supplement>.

Author contributions. All authors developed the thematic idea of the study. FL performed the numerical simulations and processed the data. GR participated in developing the model and supervised the writing of the article. FL, ML and GR interpreted the results. FL, GR, ML and HD each edited the article.

Competing interests. The contact author has declared that none of the authors has any competing interests.

Disclaimer. Publisher's note: Copernicus Publications remains neutral with regard to jurisdictional claims in published maps and institutional affiliations.

Acknowledgements. We thank the anonymous reviewer and Sven Schippkus for the helpful comments on our manuscript and editor Michal Malinowski for the editorial handling. We thank the German Federal Ministry for Economic Affairs and Climate Action (grant no. 0324360) and ESWE Innovations- und Klimaschutzfonds for their support.

Financial support. This research has been supported by the Bundesministerium für Wirtschaft und Energie (grant no. 0324360).

This open-access publication was funded by the Goethe University Frankfurt.

Review statement. This paper was edited by Michal Malinowski and reviewed by Sven Schippkus and one anonymous referee.

References

- Abreu, R., Peter, D., and Thomas, C.: Reduction of wind-turbine-generated seismic noise with structural measures, *Wind Energ. Sci.*, 7, 1227–1239, <https://doi.org/10.5194/wes-7-1227-2022>, 2022.
- Afanasiev, M., Boehm, C., van Driel, M., Krischer, L., Rietmann, M., May, D. A., Knepley, M. G., and Fichtner, A.: Modular and flexible spectral-element waveform modelling in two and three dimensions, *Geophys. J. Int.*, 216, 1675–1692, <https://doi.org/10.1093/gji/ggy469>, 2019 (code available at: <https://mondaic.com/docs/0.12.13/installation>).
- Barkan, D. D.: Dynamics of bases and foundations, McGraw-Hill, p. 325, ISBN 1391637461, 1962.
- Boese, C. M., Wotherspoon, L., Alvarez, M., and Malin, P.: Analysis of Anthropogenic and Natural Noise from Multi-level Borehole Seismometers in an Urban Environment, Auckland, New Zealand, *B. Seismol. Soc. Am.*, 105, 285–299, <https://doi.org/10.1785/0120130288>, 2015.
- Colombi, A., Roux, P., Guenneau, S., Gueguen, P., and Craster, R. V.: Forests as a natural seismic metamaterial: Rayleigh wave bandgaps induced by local resonances, *Sci. Rep.*, 6, 19238, <https://doi.org/10.1038/srep19238>, 2016.

- Eulenfeld, T. and Wegler, U.: Measurement of intrinsic and scattering attenuation of shear waves in two sedimentary basins and comparison to crystalline sites in Germany, *Geophys. J. Int.*, 205, 744–757, 2016.
- Gaßner, L. and Ritter, J.: Ground motion emissions due to wind turbines: observations, acoustic coupling, and attenuation relationships, *Solid Earth*, 14, 785–803, <https://doi.org/10.5194/se-14-785-2023>, 2023.
- Gortsas, T. V., Triantafyllidis, T., Chrisopoulos, S., and Polyzos, D.: Numerical modelling of micro-seismic and infrasound noise radiated by a wind turbine, *Soil Dyn. Earthq. Eng.*, 99, 108–123, <https://doi.org/10.1016/j.soildyn.2017.05.001>, 2017.
- Harris, C. R., Millman, K. J., van der Walt, S. J., Gommers, R., Virtanen, P., Cournapeau, D., Wieser, E., Taylor, J., Berg, S., Smith, N. J., Kern, R., Picus, M., Hoyer, S., van Kerkwijk, M. H., Brett, M., Haldane, A., del Río, J. F., Wiebe, M., Peterson, P., Gérard-Marchant, P., Sheppard, K., Reddy, T., Weckesser, W., Abbasi, H., Gohlke, C., and Oliphant, T. E.: Array programming with NumPy, *Nature*, 585, 357–362 <https://doi.org/10.1038/s41586-020-2649-2>, 2020 (code available at: <https://numpy.org/install/>).
- Hayashi, K.: Development of the Surface-wave Methods and Its Application to Site Investigations, PhD thesis, Kyoto University, Japan, <https://doi.org/10.14989/doctor.k13774>, 2008.
- Heuel, J. and Friederich, W.: Suppression of wind turbine noise from seismological data using nonlinear thresholding and denoising autoencoder, *J. Seismol.*, 26, 913–934, <https://doi.org/10.1007/s10950-022-10097-6>, 2022.
- Kumagai, T., Yanagibashi, T., Tsutsumi, A., Konishi, C., and Ueno, K.: Efficient surface wave method for investigation of the seabed, *Soils Found.*, 60, 648–667, 2020.
- Larose, E.: Lunar subsurface investigated from correlation of seismic noise, *Geophys. Res. Lett.*, 32, L16201, <https://doi.org/10.1029/2005GL023518>, 2005.
- Lerbs, N., Zieger, T., Ritter, J., and Korn, M.: Wind turbine induced seismic signals: the large-scale SMARTIE1 experiment and a concept to define protection radii for recording stations, *Near Surf. Geophys.*, 18, 467–482, <https://doi.org/10.1002/nsg.12109>, 2020.
- Limberger, F., Lindenfeld, M., Deckert, H., and Rumpker, G.: Seismic radiation from wind turbines: observations and analytical modeling of frequency-dependent amplitude decays, *Solid Earth*, 12, 1851–1864, <https://doi.org/10.5194/se-12-1851-2021>, 2021.
- Limberger, F., Rumpker, G., Lindenfeld, M., and Deckert, H.: Development of a numerical modelling method to predict the seismic signals generated by wind farms, *Sci. Rep.*, 12, 15516, <https://doi.org/10.21203/rs.3.rs-1621492/v1>, 2022.
- Malin, P. E., Bohnhoff, M., Blümle, F., Dresen, G., Martínez-Garzón, P., Nurlu, M., Ceken, U., Kadirioglu, F. T., Kartal, R. F., Kilic, T., and Yanik, K.: Microearthquakes preceding a M4.2 Earthquake Offshore Istanbul, *Sci. Rep.*, 8, 16176, <https://doi.org/10.1038/s41598-018-34563-9>, 2018.
- Neuffer, T. and Kremers, S.: How wind turbines affect the performance of seismic monitoring stations and networks, *Geophys. J. Int.*, 211, 1319–1327, <https://doi.org/10.1093/gji/ggx370>, 2017.
- Saccorotti, G., Piccinini, D., Cauchie, L., and Fiori, I.: Seismic Noise by Wind Farms: A Case Study from the Virgo Gravitational Wave Observatory, Italy, *B. Seismol. Soc. Am.*, 101, 568–578, <https://doi.org/10.1785/0120100203>, 2011.
- Spies, T., Schlittenhardt, J., and Schmidt, B.: Abschlussbericht für das Verbundprojekt MAGS2: Mikroseismische Aktivität geothermischer Systeme 2 (MAGS2) – Vom Einzelsystem zur großräumigen Nutzung, Bundesanstalt für Geowissenschaften und Rohstoffe, https://www.bgr.bund.de/MAGS/DE/Home/MAGS_node.html (last access; 15 August 2023), 2017.
- Stammler, K. and Ceranna, L.: Influence of Wind Turbines on Seismic Records of the Gräfenberg Array, *Seismol. Res. Lett.*, 87, 1075–1081, <https://doi.org/10.1785/0220160049>, 2016.
- Virtanen, P., Gommers, R., Oliphant, T. E., Haberland, M., Reddy, T., Cournapeau, D., Burovski, E., Peterson, P., Weckesser, W., Bright, J., van der Walt, S. J., Brett, M., Wilson, J., Millman, K. J., Mayorov, N., Nelson, A. R. J., Jones, E., Kern, R., Larson, E., Carey, C. J., Polat, I., Feng, Y., Moore, E. W., Vanderplas, J., Laxalde, D., Perktold, J., Cimrman, R., Henriksen, I., Quintero, E. A., Harris, C. R., Archibald, A. M., Ribeiro, A. H., Pedregosa, F., van Mulbregt, P., and SciPy 1.0 Contributors: SciPy 1.0: Fundamental Algorithms for Scientific Computing in Python, *Nat. Methods*, 17, 261–272, <https://doi.org/10.1038/s41592-020-0772-5>, 2020 (code available at: <https://scipy.org/install/>).
- Withers, M. M., Aster, R. C., Young, C. J., and Chael, E. P.: High-frequency analysis of seismic background noise as a function of wind speed and shallow depth, *B. Seismol. Soc. Am.*, 86, 1507–1515, <https://doi.org/10.1785/bssa0860051507>, 1996.
- Zieger, T. and Ritter, J. R.: Influence of wind turbines on seismic stations in the upper rhine graben, SW Germany, *J. Seismol.*, 22, 105–122, <https://doi.org/10.1007/s10950-017-9694-9>, 2018.
- Zieger, T., Nagel, S., Lutzmann, P., Kaufmann, I., Ritter, J., Ummenhofer, T., Knödel, P., and Fischer, P.: Simultaneous identification of wind turbine vibrations by using seismic data, elastic modeling and laser Doppler vibrometry, *Wind Energy*, 23, 1145–1153, <https://doi.org/10.1002/we.2479>, 2020.